

Published in final edited form as:

*Acta Biomater.* 2016 May ; 36: 310–322. doi:10.1016/j.actbio.2016.03.010.

## Assessment of a polyelectrolyte multilayer film coating loaded with BMP-2 on titanium and PEEK implants in the rabbit femoral condyle

R. Guillot<sup>1,2</sup>, I. Pignot-Paintrand<sup>1,2</sup>, J. Lavaud<sup>3</sup>, A. Decambron<sup>4,5</sup>, E. Bourgeois<sup>1,2</sup>, V. Josserand<sup>3</sup>, D. Logeart-Avramoglou<sup>4,5</sup>, E. Viguié<sup>6</sup>, and C. Picart<sup>1,2,\*</sup>

<sup>1</sup>CNRS, UMR 5628, LMGP, 3 parvis Louis Néel, F-38016 Grenoble, France

<sup>2</sup>Université de Grenoble Alpes, Grenoble Institute of Technology, 3 parvis Louis Néel, F-38016, Grenoble, France

<sup>3</sup>Institute Albert Bonniot, INSERM U823, ERL CNRS3148, Grenoble, France

<sup>4</sup>CNRS, UMR 7052, B2OA, University Paris Diderot, Sorbonne Paris Cité, F-75010, Paris, France

<sup>5</sup>Université Paris-Est, Ecole Nationale Vétérinaire d'Alfort, Maisons-Alfort Cedex, France

<sup>6</sup>ICE, UPSP 2011.03.101, Campus vétérinaire de Lyon, VetAgro Sup, Marcy l'étoile, 69280, France

### Abstract

The aim of this study was to evaluate the osseointegration of titanium implants (Ti-6Al-4V, noted here TA6V) and poly(etheretherketone) PEEK implants induced by a BMP-2-delivering surface coating made of polyelectrolyte multilayer films. The *in vitro* bioactivity of the polyelectrolyte film-coated implants was assessed using the alkaline phosphatase assay. BMP-2-coated TA6V and PEEK implants with a total dose of 9.3 µg of BMP-2 were inserted into the femoral condyles of New Zealand white rabbits and compared to uncoated implants. Rabbits were sacrificed 4 and 8 weeks after implantation. Histomorphometric analyses on TA6V and PEEK implants and microcomputed tomography on PEEK implants revealed that the bone-to-implant contact and bone area around the implants were significantly lower for the BMP-2-coated implants than for the bare implants. This was confirmed by scanning electron microscopy imaging. This difference was more pronounced at 4 weeks in comparison to the 8-week time point. However, bone growth inside the hexagonal upper hollow cavity of the screws was higher in the case of the BMP-2 coated implants. Overall, this study shows that a high dose of BMP-2 leads to localized and temporary bone impairment, and that the dose of BMP-2 delivered at the surface of an implant needs to be carefully optimized.

---

\*Corresponding author: catherine.picart@grenoble-inp.fr, phone: +33(0)4 56 52 93 11, fax: +33(0)4 56 52 93 01.

**Author Disclosure Statement.** The authors declare no competing financial interest.

## Keywords

Bone morphogenetic protein 2; orthopedic implant; osseointegration; osteoinduction; drug delivery

---

## 1 Introduction

In the field of dentistry and orthopedics, the long-term success of implant-supported prostheses largely depends on rapid healing with safe integration into the bone. Additionally, achieving a solid and rapid osseointegration is necessary for early or immediate loading of the devices, which has strong implications for decreased patient morbidity, patient psychology and health care costs. The surface properties of the implant material are key factors for rapid and stable bone tissue integration.

Titanium and its alloys, such as Ti-6Al-4V (noted hereafter TA6V), are widely used materials to manufacture dental and joint prostheses, in view of their desirable mechanical properties, chemical stability and biocompatibility [1, 2]. Several physical and chemical surface treatments have already been proposed to improve and/or speed up a reliable osseointegration of titanium implants with the aim of enhancing clinical performances [3–7]. Chemical modifications rely on acid etching [8], anodization [9] or chemical grafting [10] and physical treatments aim at changing the micrometer or nanometer scale surface roughness with a high degree of precision [11, 12].

Synthetic polymers are increasingly used as alternatives to titanium in view of their lower mechanical properties and highly tunable properties in terms of molding, processing and *in vivo* imaging [13, 14]. Poly(etheretherketone) (PEEK) is commonly used in orthopedics and spine surgery in the form of cages and screws [15]. In terms of biocompatibility and osseointegration, PEEK is considered as a bioinert material [15, 16] with a low surface energy and limited cellular adhesion [17] in comparison to titanium [18]. Besides, *in vivo* studies performed using spine cages have shown that the direct contact between PEEK implants and bone was lower than with titanium cages [19]. Several strategies have been attempted to improve the biocompatibility and osseointegration properties of PEEK, by forming bulk composites with hydroxyapatite (HAP) [20, 21], applying chemical treatments such as plasma [16, 22] or coating implants with HAP [23, 24], titanium [25], gold [26] or diamond [27]. Indeed, they were successful in improving bone growth at the PEEK surface.

Improving the surface bioactivity in an active manner via delivery of an osteoinductive agent is an even more challenging goal. Bone morphogenetic proteins (BMPs) have been introduced in human clinical practice in 2003 to induce bone formation by recruiting stem cells [28]. In particular, bone morphogenetic protein 2 (BMP-2) has been widely studied [14, 29] and is currently used in clinical devices such as collagen sponges or pastes due to its high osteoinductivity. Recently, several concerns have been raised regarding the occurrence of adverse effects of BMP-2 such as ectopic ossification, inflammatory reaction and pain [30]. The main reason for these effects is the use of a supraphysiological dose of BMP-2 (e.g. several milligrams). There is a need to engineer new delivery systems for BMP-2 [14, 29].

Coating the surface of implants was thus considered in order to localize the protein at the material surface [31].

Unfortunately, both TA6V and PEEK have a low affinity for BMP-2 and direct grafting or adsorption of BMP-2 at the implant surface leads to very low delivery of the protein or protein denaturation. In order to increase the affinity between BMP-2 and TA6V surfaces, biomimetic coatings made of HAP [32] or of biopolymers [33, 34] were developed. To date strategies to deliver BMPs from the PEEK surface are still rare. Recently, Koh and coworkers [35] created a nanoporous TiO<sub>2</sub> surface coating to immobilize BMP-2 at the PEEK surface in the nanopores.

These formulations are promising because of the similarity of HAP and biopolymers with bone tissue constituents. The underlying strategy is that a biomimetic or a nanoporous matrix can trap, retain, and deliver BMPs locally in a more efficient manner.

The layer-by-layer technique appears to be an alternative strategy because it allows to build thin polyelectrolyte multilayer films (PEM) on any kind of material substrate with precise control of various parameters such as film chemical composition, architecture, thickness (from few nm to several  $\mu\text{m}$ ) [36]. BMP-2 can be alternately assembled with hydrolytically degradable synthetic polymers to form a degradable PEM film releasing tunable doses of BMP-2 [37]. Recently, we have developed an osteoinductive PEM film coating made by assembly of poly(L-lysine) (PLL) and hyaluronan (HA), which is post-loaded with BMP-2 [38]. BMP-2 is trapped in the micrometer thick film and is locally delivered to cells [38]. Our preliminary studies showed that the PEM films deposited on tricalcium phosphate/HAP granules and on TA6V cylinders induced bone formation *in vivo* in a rat ectopic model [39, 40]. Furthermore, the film coating can be sterilized using gamma-irradiation and the shelf-life stability of BMP-2-containing films is preserved for at least one year [40].

The objective of the present study was to assess the osseointegration of BMP-2-coated TA6V and PEEK screws implanted in rabbit femoral condyles compared to uncoated - bare - implants. Since screw implantation is a common implant model to assess implant osseointegration [12, 41], we custom-designed the screws for rabbits, based on commercially available dental screws, then coated them with the BMP-2-loaded PEM films and implanted them for 4 and 8 weeks in the rabbit femoral condyle. The bone-to-implant contact and bone volume around the TA6V and PEEK screws were quantified using both histomorphometry and microcomputed tomography ( $\mu\text{CT}$ ) analyses.

## 2 Materials and Methods

### 2.1 Implant preparation

Titanium alloy (TA6V ELI, Extra Low Interstitials for clinical grade, according to norm ISO 5832-3 from HEPTAL, Neuilly-sur-Seine, France) and PEEK (TECAPEEK classix, medical implantable grade, Ensiger, Beynox France) implants were custom-made by PorteVet (France). They were specially designed for this study based on existing dental implants for clinical use in humans (Fig 1A,B). Screw shaped implants with an upper diameter of 3.8 mm and a length of 7 mm were machined (PorteVet, France). A central hole was drilled along

the vertical axis of the implant, below the hexagonal hollow cavity, to allow the screwing. Furthermore, two transversal holes were drilled along the width to assess bone formation inside the implant. These axial and transversal holes were 800  $\mu\text{m}$  in diameter. All implants were cleaned using ethanol and sterilized by steam autoclave. For bare implants, no additional process was applied. For polyelectrolyte multilayer film-coated implants, after the film-coating and BMP-2 loading (see part 2.2), the film-coated implants were additionally sterilized by UV-irradiation under a cell culture hood for 20 min.

## 2.2 Polyelectrolyte multilayer film deposition on TA6V and PEEK implants

PEM film deposition was performed using polyethyleneimine (PEI, Sigma, France) at 2 mg/mL, poly(L-lysine) hydrobromide (PLL, 55 kDa Sigma, France) at 0.5 mg/mL, and hyaluronic acid (HA 360 kDa, Lifecore, USA) at 1mg/mL dissolved in a buffered saline solution (0.15 M NaCl, 20 mM HEPES pH 7.4, called hereafter HEPES-NaCl buffer). The (PLL/HA)<sub>24</sub> films (i.e. made of 24 pairs of layer, each pair containing a PLL layer and a HA layer) were built up using an automatic dipping machine (Dipping Robot DR3, Kierstein GmbH, Germany) [40]. One layer pair of (PEI/HA) was used to enhance the PEM film adhesion onto the implant surface and the subsequent cross-linking was performed. The film-coated implants were incubated overnight at 4°C in a cross-linking solution containing 10 mg/mL of carbodiimide hydrochloride (EDC, Sigma, France) and 11 mg/mL of N-hydroxysulfosuccinimide (sulfo-NHS, Chemrio, China) in a 0.15 M NaCl solution of pH 5.5 [38, 39]. After crosslinking, the implants were roughly rinsed with HEPES-NaCl buffer and sterilized under UV.

The BMP-2 was loaded in the (PLL/HA)<sub>24</sub> films as previously described [39], the coated implants being incubated with the BMP-2 solution at 100  $\mu\text{g}/\text{mL}$  for 90 min at 37°C. The amount of BMP-2 adsorbed in the film and then released from it after immersion in the HEPES-NaCl buffer was quantified by fluorescence spectroscopy using fluorescently labeled BMP-2 [39]. Films were dried after washing twice with the HEPES-NaCl buffer for 30 s and once in ultrapure water for 5 s. The film-coated implants were further dried for 2 h under laminar airflow and were stored at 4°C until cell culture experiments or *in vivo* implantation. In total, 6 different experimental conditions with 8 implants per condition were studied (Table 1): at time point 4 weeks (two different materials TA6V and PEEK that were either bare or film-coated) and at time point 8 weeks (for PEEK only with bare or film-coated implants).

## 2.3 In vitro BMP-2 bioactivity assay

Murine C2C12 skeletal myoblasts (< 25 passages, obtained from the American Type Culture Collection, ATCC) were cultured in tissue culture Petri dishes, in a 1:1 Dulbecco's Modified Eagle Medium (DMEM):Ham's F12 medium (Gibco, Invitrogen, France) supplemented with 10% fetal bovine serum (FBS, Hyclone, USA) and 100 UI/mL penicillin G and 100 mg/mL streptomycin (Gibco, Invitrogen, France) in a 37°C, 5% CO<sub>2</sub> incubator. This medium is named hereafter C2C12 Growth Medium (GM). The bioactivity of BMP-2 on C2C12 cells was determined by assaying the BMP-2-induced alkaline phosphatase (ALP) expression, which is an early marker of osteogenic differentiation [42]. To do so, 90,000 C2C12 cells were suspended in 1 ml of GM and loaded on each implant deposited in a 48-

well cell culture plate (1 implant per well). After 3 days of culture, the implants were removed from the wells, washed with PBS, and cells were lysed by sonication over 5 s in 500  $\mu$ L of 0.1% Triton-X100 in PBS. The ALP activity of these lysates was then quantified using standard protocol [38] and normalized to the corresponding total protein content, which was determined using a bicinchoninic acid protein assay kit (Interchim, France). 3 samples (triplicate) were used for each tested condition or control and the experiment was reproduced two times.

## 2.4 Surgical implantation

TA6V or PEEK implants with or without BMP-2 were inserted into the left and right femur of rabbits in a blind manner. Each rabbit received one type of implant (TA6V or PEEK) and one implant per leg (with and without BMP-2). The veterinarian carried out the surgery without knowing which leg contained the BMP-2-coated implant. The animal experimentation was performed under the authorization of the ethical committee of Vetagro Sup (C2EA - 18, reference n° 1343) in accordance with European legislation. Twenty-four male adult New Zealand rabbits (5 months of age, 3.7 kg on average) were provided by Centre Lago (Vonnas, France), kept 2 weeks for acclimation in individual boxes with a hiding spot, a biting block and hay. Based on their age, these rabbits can be considered as adult rabbits with mature bones [50, 51]. One hour before surgery, the animals received subcutaneous (SC) injection of Borgal<sup>®</sup> (sulfadoxine and trimethoprim) 30 mg/kg, morphine 1 mg/kg and Meloxidyl<sup>®</sup> (meloxicam) 0.4 mg/kg. The anaesthesia was induced by Ketamine 1000<sup>®</sup> 40 mg/kg intra-muscularly (IM), Domitor<sup>®</sup> (medetomidine) 80  $\mu$ g/kg IM and maintained with isoflurane 1-3.5% in oxygen. After careful shaving and disinfection (Vetedine<sup>®</sup> solution and soap), the distal femoral metaphysis was surgically exposed by incisions through the skin, fascia lata (IT band) and periosteum elevation (Fig 1C). The periosteum is elevated by performing a full-layer incision in the periosteum with a #11-blade then using a periosteal elevator the periosteum is gently dissected from the bone. The flat surface on the lateral condyle of the femur was selected for implant placement. The implants were manually screwed after drilling a hole of 2.7 mm diameter and 8 mm depth using a low speed drill and profuse saline irrigation and specific taping. Before suturing the fascia lata, subcutaneous tissues and skin were flushed with sterile 150 mM NaCl solution. Just after the surgery, an X-ray scan was performed to control the position of the implant (Fig 1C'). Two hours after the surgery, injections of buprenorphine at 0.01 mg/kg (Schering-Plough, Belgium) were administered and continued at 0.005 mg/kg for three days. Borgal<sup>®</sup> 15 mg/kg IM bid. was also injected for three days. Anaesthesia recovery was performed in a quiet room (29°C) under clinical control. After the surgery, the rabbits were kept in separate cages. They had free access to tap water and were fed with pellets and hay. At 4 or 8 weeks, the rabbits were sacrificed via injection of lethal doses of sodium pentobarbital (Sanofi-Aventis, Paris, France) and the rabbit condyles were explanted and fixed in 10 % neutral formalin buffer (0.05 M phosphate buffer at pH 7.2 containing 4% w/v formaldehyde).

## 2.5 Macroscopic examination of explants

After sacrifice of the rabbits, the gross morphology of the implantation site as well as the macroscopic bone formation were examined in a blind manner by one observer, the veterinarian. The bone around the TA6V and PEEK implants was photographed using a

digital camera. The veterinarian assessed whether the implant was still visible (ie “uncovered” implants) if it was coated by the newly grown bone (so-called “covered implants”). He also assessed whether the implant had bone tissue forming in the upper hexagonal cavity of the implant. If that was the case, the implants were considered as “filled implants”. At the end of the analysis part, once we unraveled which implant was in which experimental group, we counted to total number of “covered” implants and “filled” implants in each of the six experimental groups (with  $n = 8$  implant in each group).

In addition, a score for the new bone formation (bone formation score) on the lateral part of the femoral trochlear was calculated using Osirix software (Pixmeo, Geneva, Switzerland): 0) no periarticular bone nodule ; 1) presence of small osteophytes no larger than the half of the trochlear ridge; 2) medium size osteophytes, whose size varied between the half and the full length of the trochlear ridge; 3) presence of large osteophytes, larger than the size of the trochlear ridge. For each experimental group, the bone formation scores of each implant of the group were added, giving a total score for each group.

## 2.6 Microcomputed analysis ( $\mu$ CT) on PEEK implants

Explanted rabbit condyles were imaged by  $\mu$ CT (VivaCT 40; ScancoMedical, Brüttsellen, Switzerland), which is a well-established technique [43], using a bone-dedicated high-resolution acquisition mode (145  $\mu$ A current; 55 kV voltage, 200 ms exposure time, and a 19  $\mu$ m isotropic voxel size). This commercial apparatus has a polychromatic X-Ray source and, as a consequence, there are strong scattering effects from the metallic surfaces causing the so-called inherent halation artefacts. For this reason,  $\mu$ CT quantification was only done on PEEK screws (with 8 implant per experimental condition, see Table 1). The bone-to-implant contact (BIC) was defined as the percentage of the external screw surface in contact with the bone tissue over the screw implant surface. It was measured by a manufacturer’s algorithm (IPL©\_titan2, ScancoMedical) using 290 and 1252 mgHA/cm<sup>3</sup> as thresholds for bone and PEEK, respectively. To evaluate the bone formed inside the implant cavity, a 293 mgHA/cm<sup>3</sup> threshold was applied and the bone volume fraction (BV/TV) was measured for the total volume of the screw cavity and also for a core (1x1x3 mm) in the upper part of the cavity (bone biopsy-like) (Fig. SI1). All the analyses were performed in a blind manner to the specific experimental conditions.

## 2.7 Histomorphometric analysis

The retrieved implants were processed for undecalcified histology [44]. After fixation, the implants were rinsed in water, dehydrated in ethanol, cleared in xylene, and embedded in methyl methacrylate as previously described [45]. Each implant was cut along its vertical axis giving 5-6 sections per implant (300  $\mu$ m of section thickness + 300  $\mu$ m of cutting blade thickness, leading to a distance between two sections of 600  $\mu$ m). The three most central sections from each specimen, which correspond to full-length sections, were kept for grinding to 100  $\mu$ m thickness, polishing, staining and histological analysis. We chose to analyze three sections per implant to improve the representativity of the histomorphometric analysis for the whole implant as well as to minimize the influence of the section plane on the BIC value [46]. Selected sections were ground to a thickness of 100  $\mu$ m, polished and stained with Stevenel blue and van Gieson Picrofuschin. The stained sections were then

imaged using a slide scanner (ScanScope, Aperio, France). The images were collected using the *Tribvn Ics* software (Tribvn, Chatillon, France) and the histomorphometry analysis was done with the NIS-Elements BR 2.30 software (Nikon). The analysis was performed blindly to the specific experimental conditions. Histological examination was performed under digital microscopy (Keyence/VHX-2000F, Keyence, France).

The different parameters extracted from the images are shown in Fig. S11. Bone-to-implant contact (BIC) and bone areas (BA) were measured in the cancellous bone compartment. The BIC-Thread (%) represents the available implant perimeter in contact with bone normalized over the implant perimeter length (both of them measured only within the thread area). Cancellous BA per tissue area was measured both in a region adjacent to the implant (BA-Thread) and within a distance of 100  $\mu\text{m}$  of the implant (BA-Periph).

## 2.8 Imaging by scanning electron microscopy (SEM)

One implant per time point and per group was used for SEM imaging (see Table 1). Following the euthanasia, an injection of 2.5% glutaraldehyde in 0.1 M sodium cacodylate pH 7.2 was performed in the femoral artery. Then the femoral condyles were trimmed and fixed in 2.5% glutaraldehyde in 0.1 M sodium cacodylate pH 7.2 (cacodylate buffer) at room temperature during 20 h. After three rinses with cacodylate buffer, the samples were post-fixed with 1% osmium tetroxide and 1.5% potassium hexacyanoferrate (II) trihydrate (P9387, Sigma) in water at 4°C during 24 h [47]. For dehydration, the samples were immersed in a series of ascending concentrations of ethanol (20%, 30%, 40%, 50%, 70%, 90%, 95%), incubating for at least 30 minutes in each concentration and then three times in ethanol 100%. Afterwards, samples were infiltrated with increasing concentrations (25%, 50%, 75%) of epoxy resin, incubating for 12 h in each concentration. Three exchanges with pure epoxy resin were done in 1 to 2 h steps. The specimens were embedded in epoxy resin and polymerized in a 60°C oven. The embedded tissues were cut to ~500  $\mu\text{m}$  slices along the screw longitudinal axis using a diamond saw (Escil). Selected central cross-sections were glued to a piece of silicon wafer, ground and polished to remove all the damage done by the diamond saw using a grinding system (ESC 300 GTC, Escil) and diamond grinding papers. Before imaging the surface of the implants, the samples were air-dried and then carbon-coated. A high contrast backscatter detector (vCD) was used to image the samples at 5 keV at a working distance of 7.3 mm and dwell time of 60  $\mu\text{s}$  [48] using a Quanta 250 Field emission gun (FEG) SEM (FEI Company).

## 2.9 Statistical analysis

Numerical results were reported as mean  $\pm$  standard error of the mean. Statistical analyses were conducted using the SigmaStat function of Sigma Plot 12.5 software. Statistical comparisons were based on an analysis of variance (ANOVA, Tukey Test) for pairwise and multiple comparisons in order to compare the groups two-by-two. The number of samples are described in §3.3. for *in vitro* assays and in Table 1 for the *in vivo* experiments. For all analyses, differences were accepted to be statistically significant at  $p < 0.05$ .

### 3 Results

#### 3.1 Deposition and bioactivity of BMP-2-containing PEM films coated on TA6V and PEEK screws

In this study, we used a screw model to assess osseointegration, which is a very common implant model [12, 41]. The screws were exactly of the same shape and dimensions but were made either with titanium or PEEK. These screws were implanted in rabbit femoral condyles (Fig. 1) in order to evaluate the osseointegration of surfaces coated with a BMP-2-loaded PEM film, compared to bare surfaces. We selected a loading concentration of BMP-2 (100  $\mu\text{g}/\text{mL}$ ) and one concentration of film crosslinking (EDC10) based on our previously published studies showing the osteoinductive properties of the film (loaded at this BMP-2 dose) in a rat ectopic site [39] [40]. In our previous studies, the PEM films were deposited on ceramic granules [39] and on titanium [40] and have been dried and sterilized by  $\gamma$ -irradiation[40]. We hypothesized that such a dose would also be sufficient to trigger bone formation locally at the implant surface in a bone site. BMP-2 loading and release from the polyelectrolyte films was quantified as previously described [40]. The initial amount of BMP-2 adsorbed within the film was  $\Gamma_1 = 11.3 \pm 0.3 \mu\text{g}/\text{cm}^2$  and 91.0  $\pm$  1.5 % of the protein was released within the first half day. Here, the total surface of the implanted screw determined by  $\mu\text{CT}$  was 0.8  $\text{cm}^2$ . Thus, the total amount of loaded BMP-2 was  $9.1 \pm 0.3 \mu\text{g}$  and the dose of BMP-2 released over the first half day was about 8.2  $\mu\text{g}$ .

The SEM images of the film-coated TA6V and PEEK implants (Fig. 2A,A',B) confirmed that the film was uniformly coating and smoothening the implant surface. For the PEEK implant (Fig. 2B), in view of its poor contrast by SEM, the presence of the film was best evidenced by scratching the film. The retention of the bioactivity of the BMP-2-loaded film onto the implants was assessed *in vitro* by quantifying the ALP activity of BMP-2-responsive cells (C2C12 skeletal myoblasts), ALP being an early marker of bone differentiation. C2C12 cells are a widely acknowledged cellular model to assess the bioactivity of BMP proteins [42] [49]. They exhibit a very clear response to BMPs with absolutely no ALP activity when there is no BMP-2 present. A clear dose response to BMP-2 can be measured using an ALP activity assay after 3 days of culture [38]. Freshly coated implants, and implants coated then stored for one week on the shelf were compared, as this storage corresponded to the conditions for the *in vivo* tests. The BMP-2-mediated ALP activity was similar for fresh and dry films regardless of the underlying TA6V or PEEK material tested (Fig. 2C). To note, the ALP signal for the bare material was null for both TA6V [40] and PEEK (data not shown). These results confirmed that the bioactivity of the BMP-2-coated implants was maintained upon drying and storage for one week.

#### 3.2 Preliminary experiment to define the experimental time points

A preliminary experiment was performed with 2 rabbits and 2 implants per rabbit (bare or film-coated, with TA6V in one rabbit and PEEK in the other one) and 6-week implantation time. We chose 5 month-old rabbit in order to have adult rabbit with mature bones [50, 51]. We observed using microcomputed analysis on PEEK, histomorphometric analysis and SEM analysis that the osseointegration of TA6V was already very high (of the order of 70% for the BIC) and much lower for PEEK (as observed by SEM). Beside, we verified the presence



of the polyelectrolyte film at the implant/tissue interface both at the external and internal sides of the screw (Fig SI2), the film thickness being around 4  $\mu\text{m}$ . We hypothesized that the effect of the polyelectrolyte multilayer surface coating may be more visible on PEEK, which was a less osteointegrated material. Therefore, we selected 2 time points (4 and 8 weeks) for this material. For TA6V, having in mind the cost of the *in vivo* experiments in rabbits and the ethical issues involved, we estimated that the 8-week time point would not bring useful information regarding osseointegration as the implant was already highly osteointegrated at 6 weeks. Therefore, we selected one single time point (4 week). The ethical committee validated our choices.

### 3.3 Gross morphological analysis of bone formation at the implantation site

Four or eight weeks after implantation, the condyles were collected, grossly examined and scored by a veterinarian (Fig. 3). All implants were still in place and well-fixed in the lateral femoral condyles. For some implants, bone formation occurred on top of the implant and sometimes fully covered the implant and even filled the hexagonal cavity. The number of implants fully covered with bone tissue was higher in the presence of BMP-2 (ratio of 136 %) than for bare implants (Table 2). The number of implants with the filled hexagonal cavity (“filled” implants) was also systematically higher for the BMP-2 conditions (ratio of 129 %) and there was no significant difference between the materials (TA6V or PEEK) (Table 2). For the PEEK implants, the number of filled implants increased between 4 and 8 weeks. The bone production score at 4 weeks was slightly higher for titanium in comparison to PEEK. For PEEK, this score increased between 4 and 8 weeks. Globally, when the data were pooled together for both TA6V and PEEK implants independently of the nature of the material (Table 2 and Fig. 3B), the percentage of covered implants and of filled implants were respectively 36% and 29 % higher for the BMP-2 conditions than for bare materials. The bone formation score was also 19 % higher in the BMP-2 conditions. Altogether, these results showed that the presence of BMP-2 on the implants led to an overgrowth of bone tissue at the implantation site.

### 3.4 Quantification of bone formation in and around TA6V and PEEK screws using histomorphometry and $\mu\text{CT}$

Bone formation was quantified in all the experimental conditions by histomorphometry. Representative whole cross-sections of each type of implant stained with Stevenel blue and van Gieson Picrofuschin (to stain for cells, extracellular components as well as mineralized tissue) are shown for bare and BMP-2 film-coated screws (Fig. 4 and Fig SI3). Higher magnification images taken inside the thread area are also shown (Fig. 5).

For bare TA6V and PEEK screws, new bone formation around the implant was observed at 4 weeks post-implantation with a maturation process reached between 4 and 8 weeks for PEEK implants (Fig. 4, upper row). Around the implant at a distance of  $\sim 500 \mu\text{m}$  from the threads, the woven bone tissue appeared homogeneous and dense with thick trabeculae (Fig. 4, upper row). When observed at higher magnification, each thread of both types of material was nearly entirely filled with bone tissue that was in close contact with the material surface (Fig. 5, upper row). Numerous osteoblasts were laying down osteoid tissue, indicating a high bone-forming activity.

In contrast, an altered bone tissue with a disorganized trabecular structure was observed around the BMP-2-loaded film-coated implants after 4 weeks (Fig. 4, lower row). The bone structure exhibited a loss of normal anisotropy and the number of trabeculae increased while their thickness decreased. However, a noticeable bone tissue maturation was observed around the film-coated PEEK implants at 8 weeks post-implantation (Fig. 4, lower row). Observations at higher magnification confirmed the immature and spongy aspect of the bone tissue that partly filled the threads with the absence of active osteoblasts laying down osteoid tissue (Fig. 5, lower row). The contact points with the implant surface were scarce.

All these qualitative observations were confirmed by histomorphometric quantification (Fig. 6). The BIC within the thread area (Fig. 6A) as well as the bone areas within both the thread (Fig. 6B) and the periphery (Fig. 6C) were significantly lower with the BMP-2 film-coated implants as compared to the bare implants ( $p < 0.05$ ). The differences were even more pronounced with TA6V ( $8.1 \pm 1.5$  versus  $50.0 \pm 4.6$  at 4 weeks for BIC-thread) as compared to PEEK ( $14.6 \pm 4.1$  versus  $40.0 \pm 4.0$  at 4 weeks for BIC-thread). Besides, in the case of PEEK, the difference between the BMP-2 film-coated and bare materials tended to decrease over time ( $34.5 \pm 2.0$  for bare versus  $20.3 \pm 2.6$  for BMP-2 at 8 weeks for BIC-Thread). BA-thread values were of the order of 54 to 69 % in the case of bare and 18 to 34% in the case of BMP-2 coating. BA-periph values were of the order of 58 to 68 % in the case of bare and 23 to 41% in the case of BMP-2 coating. Similar observations were made for the BIC total (Fig. SI4). In contrast, the upper cavity of the screw, (“biopsy” location, Fig. SI1), which is an open space, was filled with new bone tissue in significantly higher amounts with BMP-2-coated implants in comparison to the bare implants (Fig. 6D) ( $10.2 \pm 1.1$  (no BMP-2) versus  $1.6 \pm 0.4$  (with BMP-2) for TA6V at 4 weeks;  $6.7 \pm 1.0$  versus  $2.3 \pm 0.5$  for PEEK at 4 weeks and  $13.8 \pm 2.1$  versus  $9.8 \pm 3.4$  for PEEK at 8 weeks).

Only the explanted PEEK specimens were examined using  $\mu$ CT (Fig. 7) as the strong scatter effects from the TA6V implants (causing the so-called inherent halation artefacts) precluded quantitative measurements. The BIC increased over time regardless of the presence of BMP-2 and it was systematically lower in the presence of BMP-2 in comparison to the bare PEEK (26% and 16%, respectively, at 4 and 8 weeks post-implantation) (Fig. 7 A,A’), although these differences were not significant. To note, the total volume of bone tissue formed inside the hollow cavities of the screws was similar in the presence or absence of BMP-2 (Fig. SI5). However, when considering only the analysis in the upper hexagonal cavity of the screw (biopsy, see Figure SI1), the bone volume was 2-fold higher in the presence of BMP-2 compared to the control at 4 weeks post-implantation (Fig. 7B, B’). This effect was almost completely abolished at 8 weeks post-implantation.

### 3.5 SEM imaging of bone contact with TA6V and PEEK implants using SEM

Finally, explanted TA6V and PEEK samples were observed by SEM (Fig. 8). In agreement with the histological observations, for bare TA6V and PEEK screws, we observed that the bone tissue was directly in contact with the implants (Fig. 8 A,B,C). In contrast, in the case of the BMP-2-coated implants, bone tissue was not in so close contact with TA6V or PEEK surfaces (Fig. 8 D,E,F).

## 4 Discussion

Osseointegration, defined as a direct structural and functional connection between ordered, living bone and the surface of a load-carrying implant, is critical for implant stability, and is considered as a prerequisite for implant loading and long-term clinical success of endosteous implants [52]. However, such an achievement is still a clinical issue, especially in patients with impaired bone regeneration potential [5]. In the present study, we immobilized BMP-2 onto the surface of implants of two different materials using a biomimetic PEM film and examined the effect of such surface modification on implant osseointegration in a rabbit model. Screws made of TA6V or PEEK were implanted in rabbit femoral condyles, a validated model for evaluating the osseointegration potential of implants [12, 41].

We found that TA6V implants were better osseointegrated than PEEK implants (Fig 4,5): BIC values were between 30 and 50% for the bare implants, being slightly higher for the TA6V in comparison to PEEK (Fig. 6) and BA values were similar for both materials (50-60%) (Fig. 6). Our BIC values for TA6V implants were similar to those of TA6V implanted for 4 weeks in the tibia of osteoporotic rats [53] or implanted for 4 weeks in rabbit condyles [12]. The BIC values for bare PEEK were higher than those of nanoHAP-coated PEEK implanted in the femoral metaphysis of rabbits [41]. However, the BA values found in the latter study were of the same order of magnitude (40-60%) as our data. In addition, both the macroscopic morphological observations (Fig 3 and Table S11) as well as the quantitative histomorphometry (Fig 4-6) showed that TA6V implants promoted higher bone ingrowth than the PEEK ones. However, histological observations of PEEK explants did not show any sign of inflammatory reaction at the tissue level (Fig 5). Higher resolution SEM observations confirmed that the bone tissue was in contact with the TA6V implant surface uniformly, but was partially at a distance from the PEEK implants (Fig. 8). Taken all together, our findings are consistent with *in vitro* and *in vivo* results obtained recently by other groups [18, 54, 55]. A recent *in vivo* study in rabbits showed that PEEK resulted in a mild inflammatory response but did not elicit an aggressive immune response [55]. Boyan and coworkers in their recent comparative *in vitro* studies of TA6V and PEEK surfaces [18, 54] concluded that a TA6V surface promoted osteoblastic differentiation and fostered a specific cellular environment that favored bone formation. In contrast, PEEK led to a reduced differentiation of mesenchymal stem cells and to the production of an inflammatory environment that favored fibrosis [54].

The osteoinductive properties of BMP-2 loaded into a biopolymeric film coating either ceramic granules [39] or TA6V porous cylinders [40] were previously demonstrated in a rat ectopic model. In these previous studies, BMP-2-coated materials were prepared in the same manner as in the present study and, when implanted subcutaneously, promoted consistent new bone tissue. Here, we found that the osseointegration potential was systematically higher for both bare TA6V and PEEK implants than for the BMP-2-coated implants (Fig 4,5). Thus, surprisingly, the present results provided evidence of an impaired early osseointegration of BMP-2-coated implants compared to bare implants. Bright field (Fig. 4,5) and electron microscopy (Fig. 8) imaging indicated that bone tissue was always farther from the TA6V and PEEK implant surfaces for the BMP-2 conditions in comparison to bare implants, independently of the material. The newly formed bone also appeared of lower

quality with a disorganized trabecular structure around the BMP-2-loaded film-coated implants (Fig. 4,5), in quite a contrast with the homogeneous and dense bone tissue with thick trabeculae around bare implants 4 weeks post-implantation. Data showed that the amounts of new bone tissue formed around the implants and in contact with the implants were significantly lower for all the implants coated with the BMP-2-loaded film, regardless of the substrate material, TA6V or PEEK (Fig. 6). The  $\mu$ CT data were also consistent with a lower BIC for the BMP-2-coated implants, although the differences were not significant (Fig. 7). Notably, a higher bone volume was found solely at the macroscopic level around (Fig 3) as well as inside the upper hexagonal cavity (Fig. 7) of the BMP-2-coated implants, in comparison to bare implants.

It should be noted that the number of covered and filled implants, bone production score (Fig 3) as well as the BIC, BA-Thread and BA-Periph (Fig. 6) all increased for BMP-2-coated PEEK between 4 and 8 weeks, suggesting that this bone impairment was only transient. The differences in BA-Thread and BA-Periph between BMP-2-coated and bare PEEK implants also decreased at 8 weeks compared to 4 weeks post-implantation (Fig. 6).

In this study, neither TA6V nor PEEK implants coated with the film alone (without BMP-2) were tested. In fact, we reasoned that the important controls were the implants (e.g. bare TA6V and PEEK implants without a film coating) as they are currently used clinically. Besides, the polyelectrolyte film itself did not contain any bioactive ingredient as it was not loaded with BMP-2. It is unlikely that the polyelectrolyte components of the film itself would lead to the drastic effects observed here. In our initial studies, the (PLL/HA) films themselves elicited neither osteoinductive properties nor an inflammatory response [39, 40]. In addition, the presence of the PEM film did not affect the osteoconductive properties of TA6V implants [40]. Recently, Zankovych et al. [56] studied the effect of polyelectrolyte multilayers films containing chitosan (CHI) and gelatin (GEL), respectively (CHI/HA) and (CHI/GEL) PEM films, on the osseointegration of TA6V screws in a rat condyle model. There was no significant difference in BIC and no decrease of osseointegration for film-coated implants compared to bare implants. In all groups, there was a dynamic increase in bone area from 3 to 8 weeks. The authors also found that the polyelectrolyte coating had a positive effect on the mechanical anchorage of the implant in bone [56].

Recent studies in animals showed that BMP-2 displays numerous dose-dependent properties, especially on osteoclastic activity. In fact, an osteolytic effect of BMP-2 delivered from the clinically approved collagen sponge combined with a soft tissue oedema have already been reported in the literature in clinical studies [57, 58]. Here, no marker of osteolysis has been assessed but histological observation provided evidence of a clearly altered bone tissue when BMP-2 was coated on the implants (Fig. 4,5). These observations suggest an impaired modeling process, involving a resorptive activity higher than the bone formation activity.

In our experimental conditions, a rough estimation of the local concentration of BMP-2 at the vicinity of the implant can be made. The volume of the empty space around the implant in which BMP-2 diffuses can be calculated by assuming that diffusion occurs over a certain distance. Taking an estimate of  $\sim 100$  to  $\sim 300$   $\mu\text{m}$  for this diffusion distance gives values of 12.5 to 37.5  $\mu\text{L}$  for the total diffusion volume of BMP-2 around the whole screw. Knowing

the amount of BMP-2 released (~8.2 µg), this leads to an equivalent BMP-2 local volumic concentration on the order of ~220 to 680 µg/mL. Thus, the observed impaired bone formation induced by the BMP-2-coated implants likely results from a too high local dose of BMP-2. Indeed, recent studies in animals showed that the bone resorption effect is dose-dependent and transient [59–61]. Inflammation occurrence and abnormal bone formation have been observed in rats after 2 weeks in critical-sized femoral bone defects treated with high doses of BMP-2 (> 150 µg/mL) [59] but healing improved after weeks. These effects were only observed at high concentrations with cyst-like bony shell formation and an increased number of osteoclast-like cells. Similar initial observations were made in rat calvarial defects with subsequent complete bone resolution in 4 weeks [60] and in a femoral defect in sheep using hyper-concentrated BMP-2 solutions on a collagen sponge [61]. In the latter case, the effect was also transient and progressive healing took place over the 8-week survival period. It may also be that the recovery toward a normal bone formation, which is observed here as a function of time with PEEK, could be a result of the clearance of BMP-2 from the implant surface.

Bone loss in the presence of too high BMP-2 dosages has been attributed to the activation of osteoclasts [62]. BMP-2 is known to play an important role in bone remodeling [63] by acting as a mediator of osteoblast-osteoclast interactions and by inducing osteoclast differentiation [64, 65]. The dose of BMP-2 appears thus to be a determinant parameter. Despite the apparent low dosage of BMP-2 loaded within the film (~8.2 µg), this local concentration was revealed here to be still above the threshold of BMP-2 concentration to promote optimal bone formation without inducing adverse effects. Besides, the trabecular bone architecture was found modeled over time (between the 4th and 8th week post-implantation), proving the transient aspect of the BMP-2-mediated bone formation impairment. In future studies, we envision to decrease the amount of BMP-2 loaded in the film by decreasing the initial concentration of BMP-2 in the loading solution. We will also control the released amount by tuning the EDC crosslinking extent [40], and study a more stringent *in vivo* model such as a bone critical size defect.

## Conclusions

In this study, bone formation at the surface of PEEK and TA6V implants was compared for implants coated with a BMP-2-containing film and for bare implants after 4 and 8 weeks in rabbit femoral condyles. The bone-to-implant contact and bone area around the coated implants were systematically lower than around bare implants. However, these values increased between 4 and 8 weeks for PEEK implants, indicating that this initial impairment effect on the local bone formation was only transient. In contrast, significantly more bone was formed at 4 weeks in an empty space, inside the upper hexagonal cavity of the screws for the BMP-2-coated implant. This was observed independently of the material, TA6V or PEEK. This study highlights that the local dose of BMP-2 delivered around an implant via a surface-coating is an important parameter that needs to be carefully optimized for the induction of bone growth, and therefore optimal osseointegration. It also suggests that BMP-2 may rather be indicated for the repair of large bone defects, as BMP-2 initiated bone growth in the empty space formed by the upper hexagonal cavity of the screw.

## Supplementary Material

Refer to Web version on PubMed Central for supplementary material.

## Acknowledgments

This work was supported by the European Commission (FP7 program) via European Research Council starting and proof of concept grants (BIOMIM, GA 259370 and OSCODI, GA 334966 to CP). We wish to thank Porte Vet company (France) for the fabrication of the screws, Laetitia Rapenne for her help with the sample preparation for SEM, Jean Boutonnat for his useful comments of the histological images, Olivia Leveneur for her help in the design of the *in vivo* study, Elodie Pilet for her assistance in the surgery, Hanane El Hafci for the histological processing of the samples and Marianne Bourguignon for the slide scanning.

## Bibliographic References

- [1]. Geetha M, Singh AK, Asokamani R, Gogia AK. Ti based biomaterials, the ultimate choice for orthopaedic implants - A review. *Prog Mater Sci.* 2009; 54:397–425.
- [2]. Duraccio D, Mussano F, Faga MG. Biomaterials for dental implants: current and future trends. *J Mater Sci-Mater Med.* 2015; 50:4779–812.
- [3]. Junker R, Dimakis A, Thoneick M, Jansen JA. Effects of implant surface coatings and composition on bone integration: a systematic review. *Clin Oral Implant Res.* 2009; 20:185–206.
- [4]. Wennerberg A, Albrektsson T. Effects of titanium surface topography on bone integration: a systematic review. *Clin Oral Implants Res.* 2009; 20(Suppl 4):172–84. [PubMed: 19663964]
- [5]. Palmquist A, Omar OM, Esposito M, Lausmaa J, Thomsen P. Titanium oral implants: surface characteristics, interface biology and clinical outcome. *J R Soc Interface.* 2010; 7(Suppl 5):S515–27. [PubMed: 20591849]
- [6]. Schwarz F, Herten M, Sager M, Wieland M, Dard M, Becker J. Bone regeneration in dehiscence-type defects at chemically modified (SLActive((R))) and conventional SLA titanium implants: a pilot study in dogs. *J Clin Periodontol.* 2007; 34:78–86. [PubMed: 17137467]
- [7]. Wennerberg A, Bougas K, Jimbo R, Albrektsson T. Implant coatings: new modalities for increased osseointegration. *American journal of dentistry.* 2013; 26:105–12. [PubMed: 24073534]
- [8]. Schliephake H, Aref A, Scharnweber D, Bierbaum S, Sewing A. Effect of modifications of dual acid-etched implant surfaces on peri-implant bone formation. Part I: organic coatings. *Clin Oral Implant Res.* 2009; 20:31–7.
- [9]. Walter MS, Frank MJ, Sunding MF, Gomez-Florit M, Monjo M, Bucko MM, Pamula E, Lyngstadaas SP, Haugen HJ. Increased reactivity and *in vitro* cell response of titanium based implant surfaces after anodic oxidation. *J Mater Sci Mater Med.* 2013; 24:2761–73. [PubMed: 23912792]
- [10]. Petrie TA, Raynor JE, Dumbauld DW, Lee TT, Jagtap S, Templeman KL, Collard DM, Garcia AJ. Multivalent integrin-specific ligands enhance tissue healing and biomaterial integration. *Sci Transl Med.* 2010; 2:45ra60.
- [11]. Gittens RA, Olivares-Navarrete R, Schwartz Z, Boyan BD. Implant osseointegration and the role of microroughness and nanostructures: Lessons for spine implants. *Acta Biomater.* 2014; 10:3363–71. [PubMed: 24721613]
- [12]. Salou L, Hoornaert A, Louarn G, Layrolle P. Enhanced osseointegration of titanium implants with nanostructured surfaces: an experimental study in rabbits. *Acta Biomater.* 2015; 11:494–502. [PubMed: 25449926]
- [13]. Puppi D, Chiellini F, Piras AM, Chiellini E. Polymeric materials for bone and cartilage repair. *Prog Polym Sci.* 2010; 35:403–40.
- [14]. Lo KWH, Ulery BD, Ashe KM, Laurencin CT. Studies of bone morphogenetic protein-based surgical repair. *Adv Drug Deliv Rev.* 2012; 64:1277–91. [PubMed: 22512928]
- [15]. Kurtz SM, Devine JN. PEEK biomaterials in trauma, orthopedic, and spinal implants. *Biomaterials.* 2007; 28:4845–69. [PubMed: 17686513]

- [16]. Poulsson AHC, Eglin D, Zeiter S, Camenisch K, Sprecher C, Agarwal Y, Nehrass D, Wilson J, Richards RG. Osseointegration of machined, injection moulded and oxygen plasma modified PEEK implants in a sheep model. *Biomaterials*. 2014; 35:3717–28. [PubMed: 24485795]
- [17]. Sagomonyants KB, Jarman-Smith ML, Devine JN, Aronow MS, Gronowicz GA. The in vitro response of human osteoblasts to polyetheretherketone (PEEK) substrates compared to commercially pure titanium. *Biomaterials*. 2008; 29:1563–72. [PubMed: 18199478]
- [18]. Olivares-Navarrete R, Gittens RA, Schneider JM, Hyzy SL, Haithcock DA, Ullrich PF, Schwartz Z, Boyan BD. Osteoblasts exhibit a more differentiated phenotype and increased bone morphogenetic protein production on titanium alloy substrates than on poly-ether-ether-ketone. *Spine Journal*. 2012; 12:265–72. [PubMed: 22424980]
- [19]. Toth JM, Wang M, Estes BT, Scifert JL, Seim HB, Turner AS. Polyetheretherketone as a biomaterial for spinal applications. *Biomaterials*. 2006; 27:324–34. [PubMed: 16115677]
- [20]. Abu Bakar MS, Cheng MHW, Tang SM, Yu SC, Liao K, Tan CT, Khor KA, Cheang P. Tensile properties, tension-tension fatigue and biological response of polyetheretherketone-hydroxyapatite composites for load-bearing orthopedic implants. *Biomaterials*. 2003; 24:2245–50. [PubMed: 12699660]
- [21]. Wong KL, Wong CT, Liu WC, Pan HB, Fong MK, Lam WM, Cheung WL, Tang WM, Chiu KY, Luk KDK, Lu WW. Mechanical properties and in vitro response of strontium-containing hydroxyapatite/polyetheretherketone composites. *Biomaterials*. 2009; 30:3810–7. [PubMed: 19427032]
- [22]. Zhao Y, Wong HM, Wang WH, Li PH, Xu ZS, Chong EYW, Yan CH, Yeung KWK, Chu PK. Cytocompatibility, osseointegration, and bioactivity of three-dimensional porous and nanostructured network on polyetheretherketone. *Biomaterials*. 2013; 34:9264–77. [PubMed: 24041423]
- [23]. Ha SW, Kirch M, Birchler F, Eckert KL, Mayer J, Wintermantel E, Sittig C, PfundKlingenfuss I, Textor M, Spencer ND, Guecheva M, et al. Surface activation of polyetheretherketone (PEEK) and formation of calcium phosphate coatings by precipitation. *J Mater Sci-Mater Med*. 1997; 8:683–90. [PubMed: 15348819]
- [24]. Lee JH, Jang HL, Lee KM, Baek HR, Jin K, Hong KS, Noh JH, Lee HK. In vitro and in vivo evaluation of the bioactivity of hydroxyapatite-coated polyetheretherketone biocomposites created by cold spray technology. *Acta Biomater*. 2013; 9:6177–87. [PubMed: 23212079]
- [25]. Han CM, Lee EJ, Kim HE, Koh YH, Kim KN, Ha Y, Kuh SU. The electron beam deposition of titanium on polyetheretherketone (PEEK) and the resulting enhanced biological properties. *Biomaterials*. 2010; 31:3465–70. [PubMed: 20153890]
- [26]. Yao C, Storey D, Webster TJ. Nanostructured metal coatings on polymers increase osteoblast attachment. *Int J Nanomed*. 2007; 2:487–92.
- [27]. Wang HY, Xu M, Zhang W, Kwok DTK, Jiang JA, Wu ZW, Chu PK. Mechanical and biological characteristics of diamond-like carbon coated poly aryl-ether-ether-ketone. *Biomaterials*. 2010; 31:8181–7. [PubMed: 20692699]
- [28]. Schmidmaier G, Schwabe P, Strobel C, Wildemann B. Carrier systems and application of growth factors in orthopaedics. *Injury*. 2008; 39(Suppl 2):S37–43. [PubMed: 18804572]
- [29]. Lauzon MA, Bergeron E, Marcos B, Fauchoux N. Bone repair: new developments in growth factor delivery systems and their mathematical modeling. *J Control Release*. 2012; 162:502–20. [PubMed: 22889715]
- [30]. Carragee EJ, Hurwitz EL, Weiner BK. A critical review of recombinant human bone morphogenetic protein-2 trials in spinal surgery: emerging safety concerns and lessons learned. *Spine J*. 2011; 11:471–91. [PubMed: 21729796]
- [31]. King WJ, Krebsbach PH. Growth factor delivery: how surface interactions modulate release in vitro and in vivo. *Adv Drug Deliv Rev*. 2012; 64:1239–56. [PubMed: 22433783]
- [32]. Liu Y, Enggist L, Kuffer AF, Buser D, Hunziker EB. The influence of BMP-2 and its mode of delivery on the osteoconductivity of implant surfaces during the early phase of osseointegration. *Biomaterials*. 2007; 28:2677–86. [PubMed: 17321590]

- [33]. Kim SE, Song SH, Yun YP, Choi BJ, Kwon IK, Bae MS, Moon HJ, Kwon YD. The effect of immobilization of heparin and bone morphogenic protein-2 (BMP-2) to titanium surfaces on inflammation and osteoblast function. *Biomaterials*. 2011; 32:366–73. [PubMed: 20880582]
- [34]. Schliephake H, Aref A, Scharnweber D, Bierbaum S, Roessler S, Sewing A. Effect of immobilized bone morphogenic protein 2 coating of titanium implants on peri-implant bone formation. *Clin Oral Implants Res*. 2005; 16:563–9. [PubMed: 16164462]
- [35]. Han CM, Jang TS, Kim HE, Koh YH. Creation of nanoporous TiO<sub>2</sub> surface onto polyetheretherketone for effective immobilization and delivery of bone morphogenetic protein. *J Biomed Mater Res A*. 2014; 102:793–800. [PubMed: 23589347]
- [36]. Boudou T, Crouzier T, Ren K, Blin G, Picart C. Multiple functionalities of polyelectrolyte multilayer films: new biomedical applications. *Adv Mater*. 2010; 22:441–67. [PubMed: 20217734]
- [37]. Shah NJ, Hyder MN, Moskowitz JS, Quadir MA, Morton SW, Seeherman HJ, Padera RF, Spector M, Hammond PT. Surface-mediated bone tissue morphogenesis from tunable nanolayered implant coatings. *Sci Transl Med*. 2013; 5:10.
- [38]. Crouzier T, Ren K, Nicolas C, Roy C, Picart C. Layer-by-Layer films as a biomimetic reservoir for rhBMP-2 delivery: controlled differentiation of myoblasts to osteoblasts. *Small*. 2009; 5:598–608. [PubMed: 19219837]
- [39]. Crouzier T, Sailhan F, Becquart P, Guillot R, Logeart-Avramoglou D, Picart C. The performance of BMP-2 loaded TCP/HAP porous ceramics with a polyelectrolyte multilayer film coating. *Biomaterials*. 2011; 32:7543–54. [PubMed: 21783243]
- [40]. Guillot R, Gilde F, Becquart P, Sailhan F, Lapeyriere A, Logeart-Avramoglou D, Picart C. The stability of BMP loaded polyelectrolyte multilayer coatings on titanium. *Biomaterials*. 2013; 34:5737–46. [PubMed: 23642539]
- [41]. Barkarmo S, Wennerberg A, Hoffman M, Kjellin P, Breiding K, Handa P, Stenport V. Nano-hydroxyapatite-coated PEEK implants: A pilot study in rabbit bone. *J Biomed Mater Res Part A*. 2013; 101:465–71.
- [42]. Katagiri T, Yamaguchi A, Komaki M, Abe E, Takahashi N, Ikeda T, Rosen V, Wozney JM, Fujisawa-Sehara A, Suda T. Bone morphogenetic protein-2 converts the differentiation pathway of C2C12 myoblasts into the osteoblast lineage. *J Cell Biol*. 1994; 127:1755–66. [PubMed: 7798324]
- [43]. Bouxsein ML, Boyd SK, Christiansen BA, Guldberg RE, Jepsen KJ, Muller R. Guidelines for assessment of bone microstructure in rodents using micro-computed tomography. *Journal of bone and mineral research : the official journal of the American Society for Bone and Mineral Research*. 2010; 25:1468–86.
- [44]. Murice-Lambert E, Banford AB, Folger RL. Histological preparation of implanted biomaterials for light microscopic evaluation of the implant-tissue interaction. *Stain Technol*. 1989; 64:19–24. [PubMed: 2662476]
- [45]. Guillemain G, Meunier A, Dallant P, Christel P, Pouliquen JC, Sedel L. Comparison of coral resorption and bone apposition with two natural corals of different porosities. *J Biomed Mater Res*. 1989; 23:765–79. [PubMed: 2738087]
- [46]. Kopp S, Warkentin M, Ori F, Ottl P, Kundt G, Frerich B. Section plane selection influences the results of histomorphometric studies: the example of dental implants. *Biomedizinische Technik Biomedical engineering*. 2012; 57:365–70. [PubMed: 25854664]
- [47]. Cribb B, Armstrong W, Whittington I. Simultaneous fixation using glutaraldehyde and osmium tetroxide or potassium ferricyanide-reduced osmium for the preservation of monogenean flatworms: An assessment for Merizocotyle icopae. *Microsc Res Tech*. 2004; 63:102–10. [PubMed: 14722907]
- [48]. Hekking LH, Lebbink MN, De Winter DA, Schneijdenberg CT, Brand CM, Humbel BM, Verkleij AJ, Post JA. Focused ion beam-scanning electron microscope: exploring large volumes of atherosclerotic tissue. *Journal of microscopy*. 2009; 235:336–47. [PubMed: 19754727]
- [49]. Cheng H, Jiang W, Phillips FM, Haydon RC, Peng Y, Zhou L, Luu HH, An N, Breyer B, Vanichakarn P, Szatkowski JP, et al. Osteogenic activity of the fourteen types of human bone



- morphogenetic proteins (BMPs). *J Bone Joint Surg-Am.* 2003; 85:1544–52. [PubMed: 12925636]
- [50]. Kaweblum M, Aguilar MC, Blancas E, Kaweblum J, Lehman WB, Grant AD, Strongwater AM. Histological and radiographic determination of the age of physeal closure of the distal femur, proximal tibia, and proximal fibula of the New Zealand white rabbit. *J Orthop Res.* 1994; 12:747–9. [PubMed: 7931793]
- [51]. Isaksson H, Harjula T, Koistinen A, Iivarinen J, Seppanen K, Arokoski JP, Brama PA, Jurvelin JS, Helminen HJ. Collagen and mineral deposition in rabbit cortical bone during maturation and growth: effects on tissue properties. *J Orthop Res.* 2010; 28:1626–33. [PubMed: 20540098]
- [52]. Anil, S.; Anand, PS.; Alghamdi, H.; Jansen, JA. Dental implant surface enhancement and osseointegration. *Implant dentistry - A rapidly evolving practice*: InTech. Turkyilmaz, PI., editor. 2011.
- [53]. Wolffe JV, Fiedler J, Durselen L, Reichert J, Scharnweber D, Forster A, Schwenzer B, Reichel H, Ignatius A, Brenner RE. Improved anchorage of Ti6Al4V orthopaedic bone implants through oligonucleotide mediated immobilization of BMP-2 in osteoporotic rats. *Plos One.* 2014; 9:7.
- [54]. Olivares-Navarrete R, Hyzy SL, Slosar PJ, Schneider JM, Schwartz Z, Boyan BD. Implant materials generate different peri-implant inflammatory factors: Poly-ether-ether-ketone promotes fibrosis and microtextured titanium promotes osteogenic factors. *Spine (Phila Pa 1976).* 2015; 40:399–404. [PubMed: 25584952]
- [55]. Hallab NJ, Bao QB, Brown T. Assessment of epidural versus intradiscal biocompatibility of PEEK implant debris: an in vivo rabbit model. *Eur Spine J.* 2013; 22:2740–51. [PubMed: 23996005]
- [56]. Zankovych S, Diefenbeck M, Bossert J, Muckley T, Schrader C, Schmidt J, Schubert H, Bischoff S, Faucon M, Finger U, Jandt KD. The effect of polyelectrolyte multilayer coated titanium alloy surfaces on implant anchorage in rats. *Acta Biomater.* 2013; 9:4926–34. [PubMed: 22902814]
- [57]. Fu RW, Selph S, McDonagh M, Peterson K, Tiwari A, Chou R, Helfand M. Effectiveness and harms of recombinant human bone morphogenetic protein-2 in spine fusion: A systematic review and meta-analysis. *Ann Intern Med.* 2013; 158:890–902. [PubMed: 23778906]
- [58]. Epstein NE. Complications due to the use of BMP/INFUSE in spine surgery: The evidence continues to mount. *Surgical neurology international.* 2013; 4:S343–52. [PubMed: 23878769]
- [59]. Zara JN, Siu RK, Zhang X, Shen J, Ngo R, Lee M, Li W, Chiang M, Chung J, Kwak J, Wu BM, et al. High doses of bone morphogenetic protein 2 induce structurally abnormal bone and inflammation in vivo. *Tissue Eng Part A.* 2011; 17:1389–99. [PubMed: 21247344]
- [60]. Pelaez M, Susin C, Lee J, Fiorini T, Bisch FC, Dixon DR, McPherson JC 3rd, Buxton AN, Wikesjo UM. Effect of rhBMP-2 dose on bone formation/maturation in a rat critical-size calvarial defect model. *J Clin Periodontol.* 2014; 41:827–36. [PubMed: 24807100]
- [61]. Toth JM, Boden SD, Burkus JK, Badura JM, Peckham SM, McKay WF. Short-term osteoclastic activity induced by locally high concentrations of recombinant human bone morphogenetic protein-2 in a cancellous bone environment. *Spine (Phila Pa 1976).* 2009; 34:539–50. [PubMed: 19240666]
- [62]. Kanatani M, Sugimoto T, Kaji H, Kobayashi T, Nishiyama K, Fukase M, Kumegawa M, Chihara K. Stimulatory effect of bone morphogenetic protein-2 on osteoclast-like cell formation and bone-resorbing activity. *J Bone Miner Res.* 1995; 10:1681–90. [PubMed: 8592944]
- [63]. Santo VE, Gomes ME, Mano JF, Reis RL. Controlled release strategies for bone, cartilage, and osteochondral engineering--Part I: recapitulation of native tissue healing and variables for the design of delivery systems. *Tissue Eng Part B Rev.* 2013; 19:308–26. [PubMed: 23268651]
- [64]. Itoh K, Udagawa N, Katagiri T, Iemura S, Ueno N, Yasuda H, Higashio K, Quinn JM, Gillespie MT, Martin TJ, Suda T, et al. Bone morphogenetic protein 2 stimulates osteoclast differentiation and survival supported by receptor activator of nuclear factor-kappaB ligand. *Endocrinology.* 2001; 142:3656–62. [PubMed: 11459815]
- [65]. Irie K, Alpaslan C, Takahashi K, Kondo Y, Izumi N, Sakakura Y, Tsuruga E, Nakajima T, Ejiri S, Ozawa H, Yajima T. Osteoclast differentiation in ectopic bone formation induced by recombinant human bone morphogenetic protein 2 (rhBMP-2). *Journal of bone and mineral metabolism.* 2003; 21:363–9. [PubMed: 14586792]

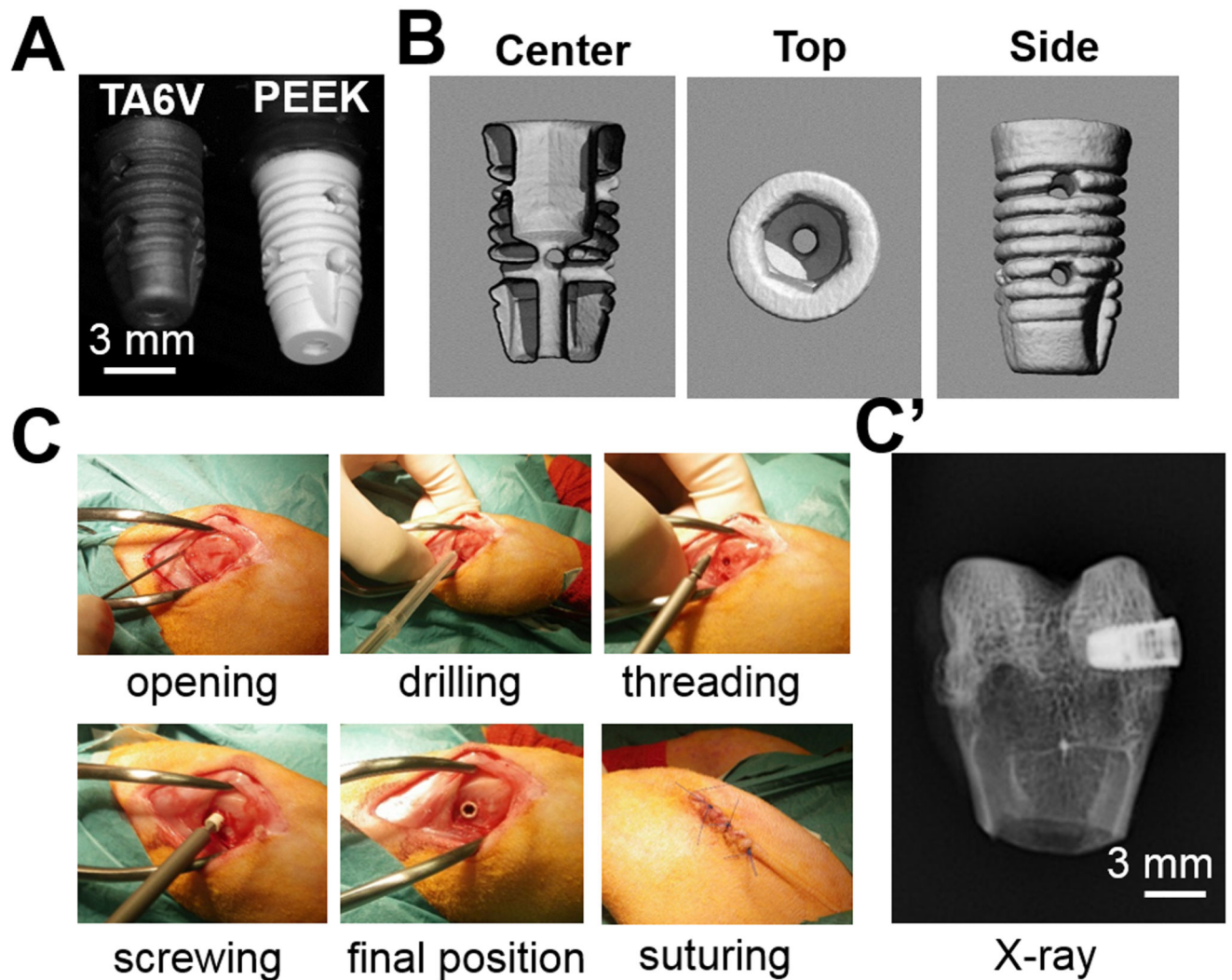


**Figure 1. Experimental design of the in vivo experiments.**

(A) Images of the PEEK and TA6V screws taken with a digital camera ; (B)  $\mu$ CT images of the PEEK screw with a center view showing hollow cross-section and top view showing the hollow hexagonal cavity in the upper part of the screw and side view showing the 2 lateral holes. (C) Different steps of the surgical procedure and (C') final placement of the implant in the rabbit condyle as imaged by X-ray.

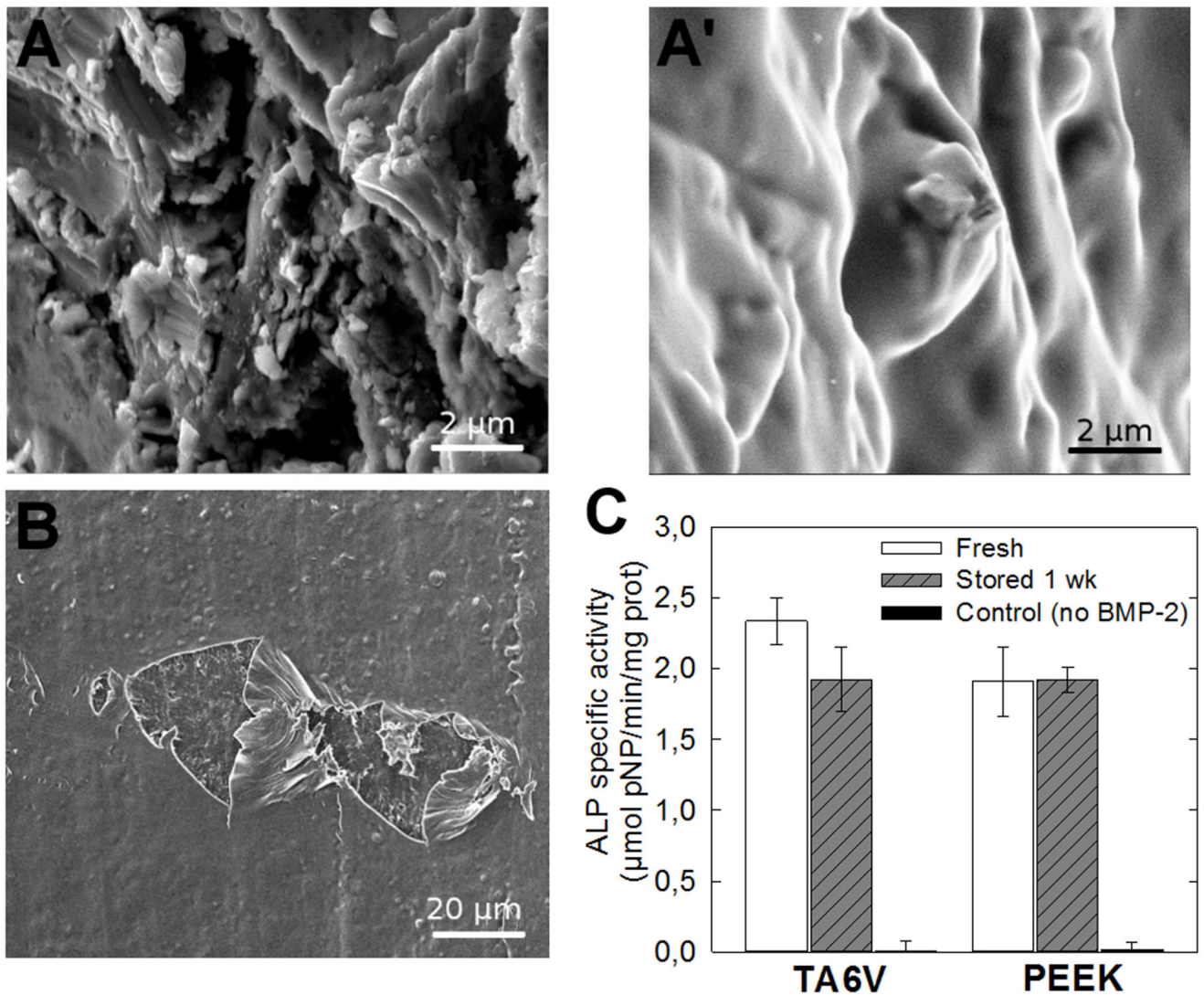


**Figure 2. Characterization of the PEM coating on TA6V and PEEK implants and *in vitro* film bioactivity.**

(A-A') Surface of the bare and PEM-coated TA6V implant imaged by SEM. (B) SEM image of the film-coated PEEK implant that was deliberately scratched in order to visualize the film and the underlying PEEK surface. (C) *In vitro* bioactivity assay of BMP-2-loaded PEM films coating TA6V and PEEK surfaces as assessed by ALP activity. The ALP test was performed on implant surfaces coated with either freshly prepared film or dry BMP-2-loaded film stored for one week on the shelf in comparison to a control implant (TA6V or PEEK with the film coating but without BMP-2). 3 samples were used for each condition and controls.

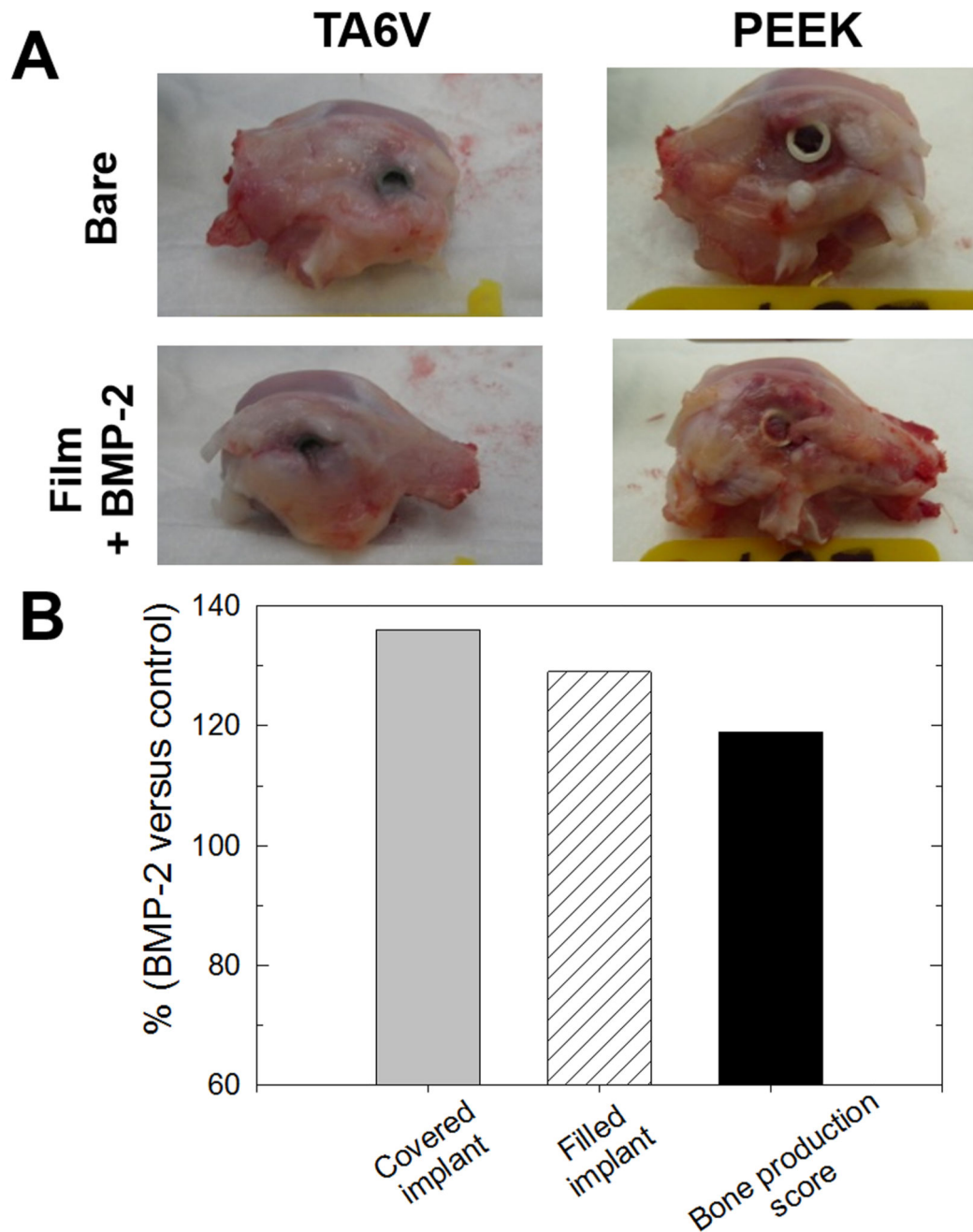


**Figure 3. Morphological observations following implantation of the screw in the rabbit femoral condyle.**

(A) Representative images of the condyles taken right after explantation for TA6V and PEEK implants (either bare or film-coated); (B) Quantification of tissue formation and bone production around the implants. The data represent the % of increase for the BMP-2-coated implants (whatever the nature of the supporting implant, TA6V or PEEK) in comparison to the bare implants (see Table 2 for full details of the calculations).

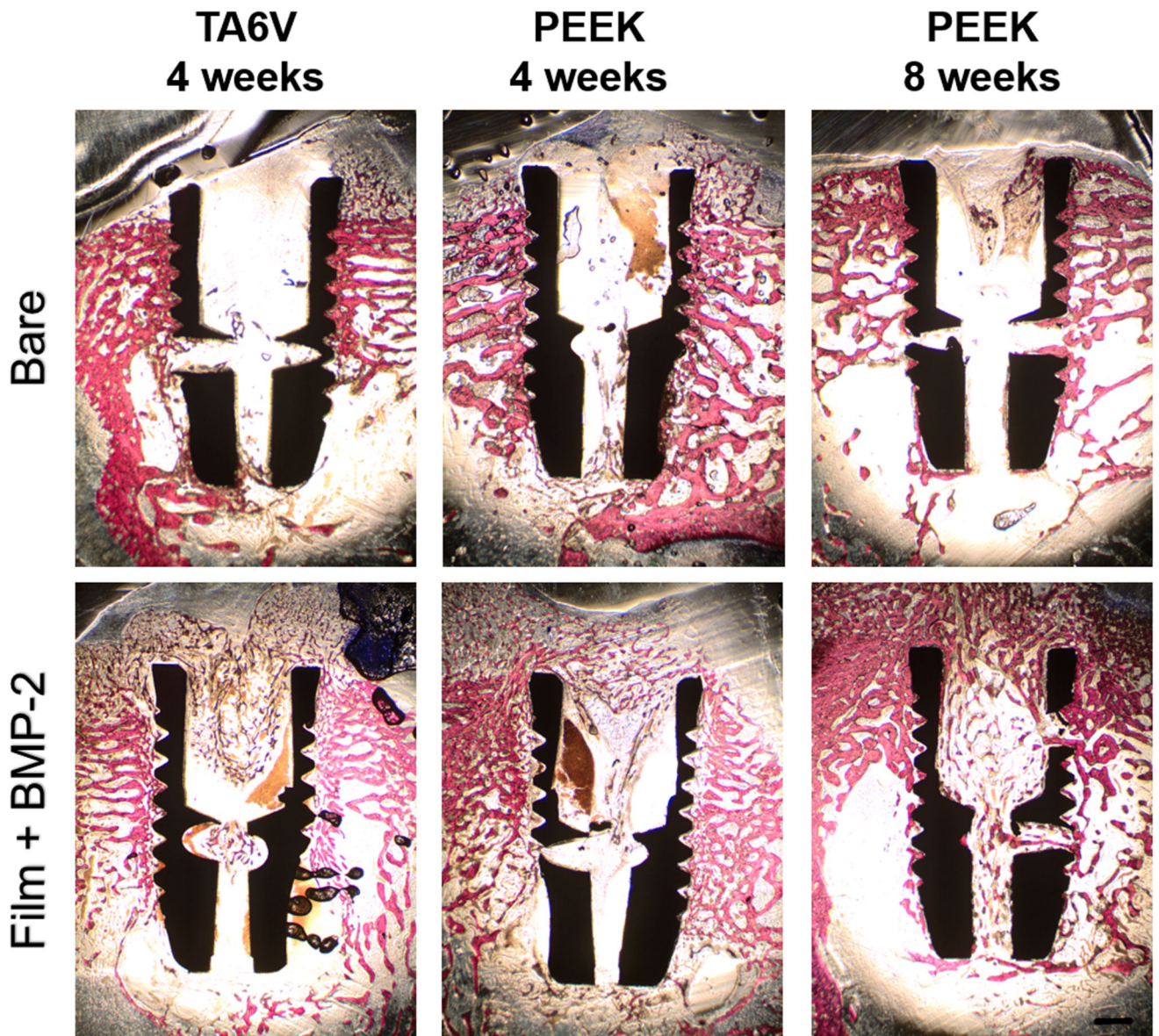


**Figure 4. Images of histological sections along the screw length.**

Representative longitudinal sections of each type of implant tested after 4 and 8 weeks of implantation and stained with Stevenel blue and van Gieson Picrofuschin. The implants appears in black, bone in pink, extracellular components and cells in blue. Differences in osseointegration between the bare and the film-coated implants can be observed: a homogeneous trabecular bone tissue was formed within the threads of both bare TA6V and PEEK implants after both 4 and 8 weeks. In contrast, an altered bone tissue with a disorganized trabecular structure was observed around the film-coated implants after 4 weeks. Bone tissue maturation was noticeable around the BMP-2 film-coated PEEK implants after 8 weeks. Scale bar: 1 mm.

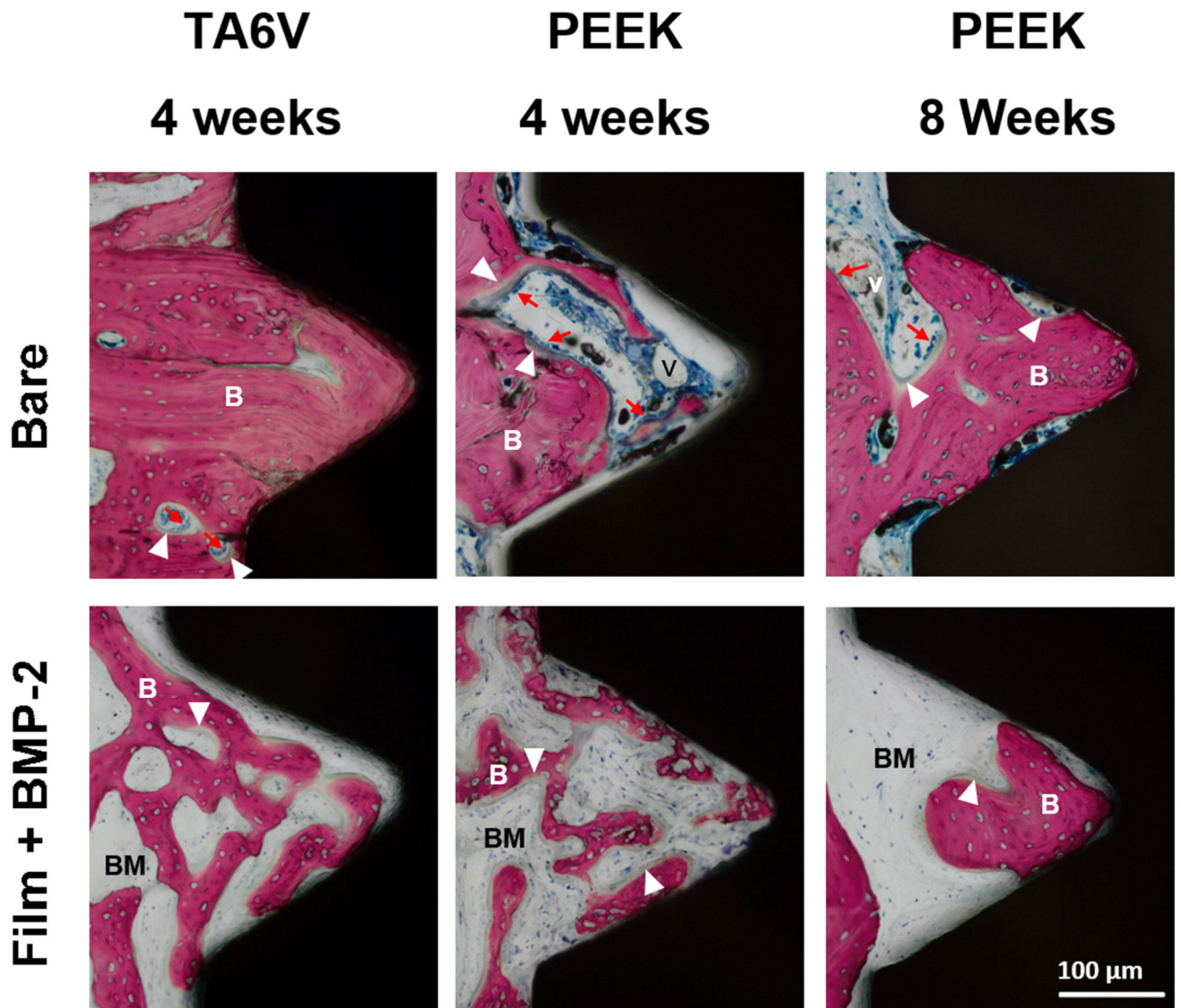


**Figure 5. Representative images of histological sections focused on a thread.**

The conditions are the same as for Figure 4. Dense woven bone entirely filled the thread of bare TA6V implants without fibrosis interposition between bone and implant as soon as 4 weeks post-implantation. Bone tissue also filled the thread of PEEK implants over time. In contrast, bone tissue within threads of BMP-2 film-coated implants appeared immature and displayed a high bone-forming activity as shown by the presence of numerous embedded osteocytes and osteoblasts laying down osteoid tissue. (scale bare 100  $\mu$ m). (B) bone tissue; (v) blood vessel; (BM) bone marrow tissue; (white arrowhead) osteoid osteoblasts; (red arrows) lining osteoblasts. (scale bare 100  $\mu$ m).

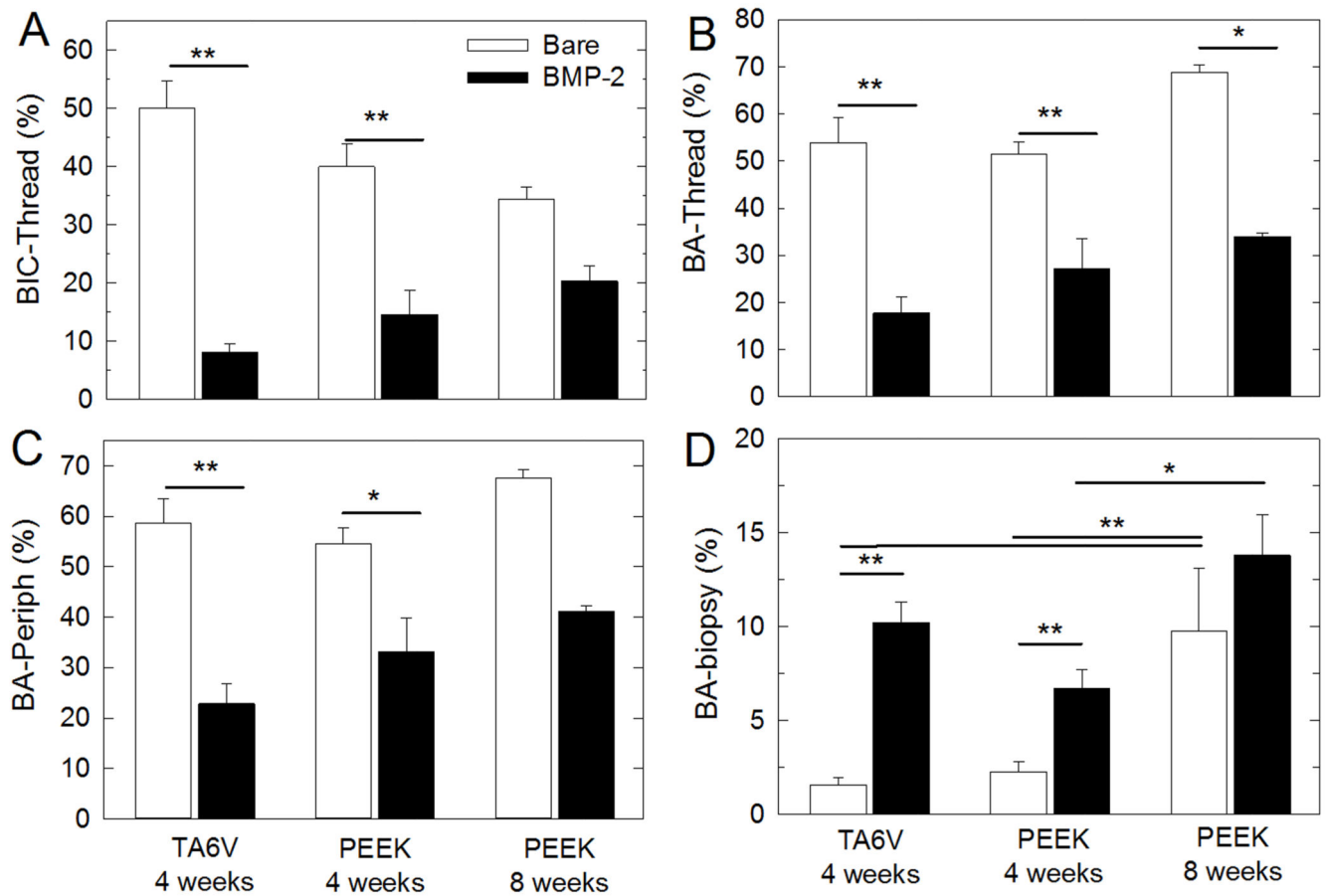


**Figure 6. Quantitative analysis of histomorphometry.**

(A) Bone-to-implant contact along the thread (BIC-Thread). Bone area (BA) inside the thread (B), at the periphery (C) and in the biopsy (D). These parameters are explained in Figure S11. Data represent 8 samples per experimental condition for the 4-week time point for PEEK and for TA6V (bare or with BMP-2), and 3 samples per condition for the 8-week time point for PEEK (bare or with BMP-2).\*: indicates significant difference (\* $p < 0.05$ , \*\*  $p < 0.001$ , Pairwise comparison Tukey test).

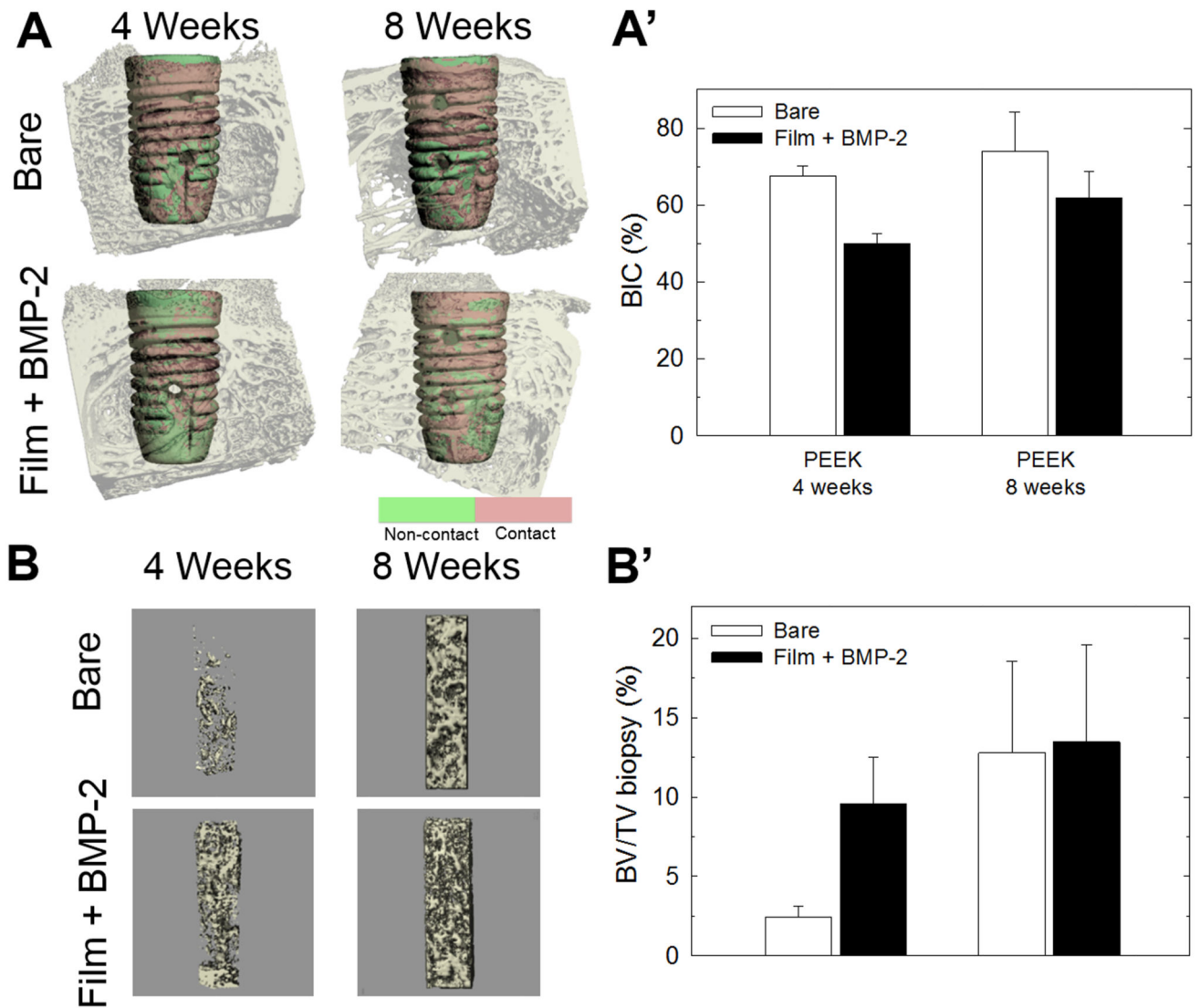


**Figure 7.  $\mu$ CT analysis of bone around and inside the cavity of the bare and film-coated PEEK screws.**

(A) Representative images of the bare and BMP-2-loaded film-coated screws taken at 4 and 8 weeks. (A') Corresponding quantitative analysis of the BIC. (B) Representative images of bone formation in a core of the upper part of the screw cavity (bone biopsy-like, see Fig S11 for the schematic). (B') Corresponding quantitative analysis of BV/TV (%). Data correspond to 8 samples per condition.



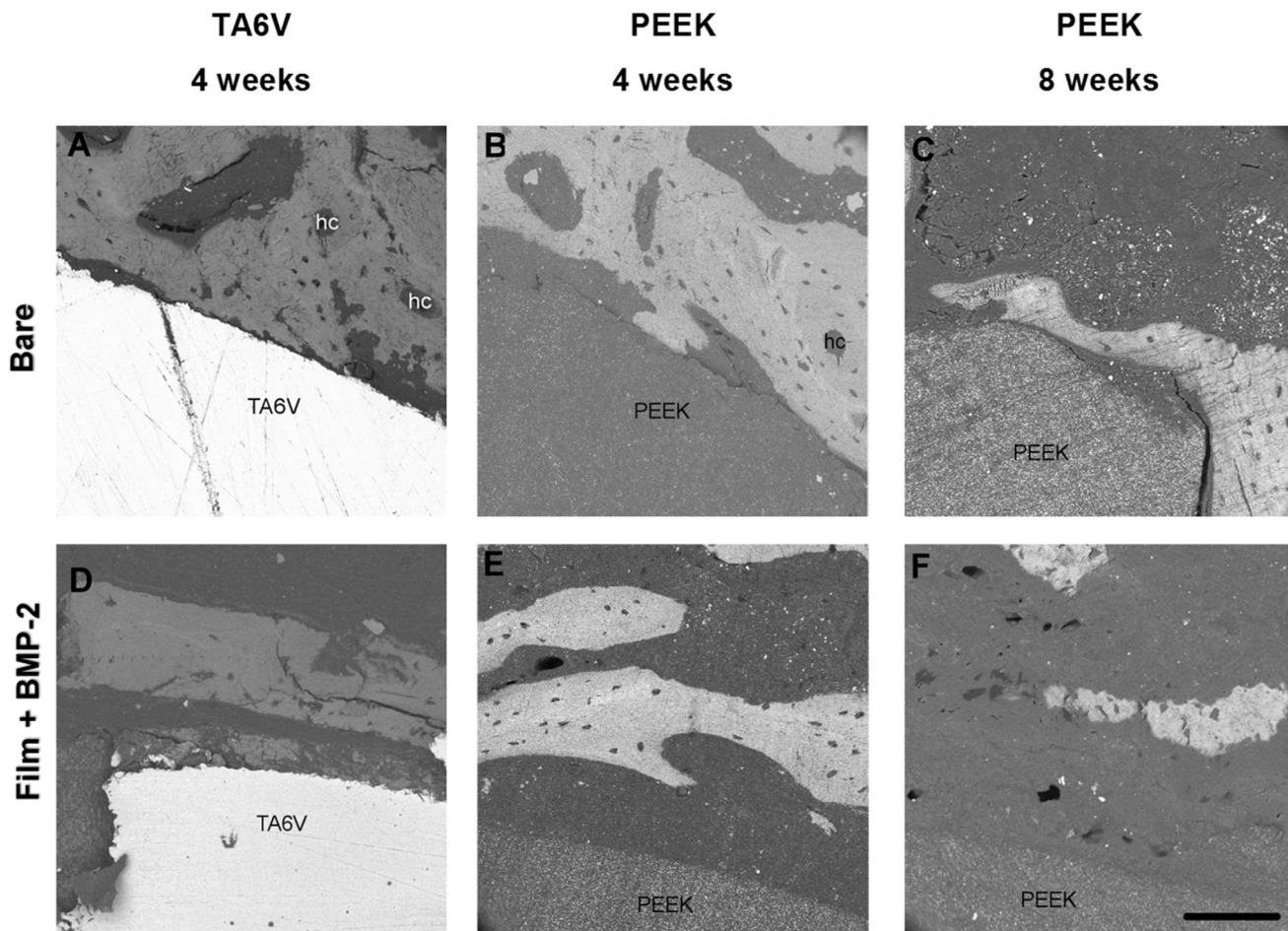


**Figure 8. SEM imaging of the bare and film-coated TA6V and PEEK screws.**

Backscattered electron (BSE) images of a transverse section of TA6V after 4 weeks and PEEK implants after 4 and 8 weeks for bare implants (A, B, C) and for the film-coated implants (D,E,F). For bare implants, the bone was directly in contact with the implant (A,B,C). The formation of osteons with haversian canals (hc) in circular shape corresponded to new bone formation (C). Note the difference in mineralization level as can be observed by the different grey levels indicating a mature bone. In the presence of BMP-2-loaded film, the bone was further away from the implant (D,E,F).